Supporting Information

Extra Long Electron-hole Diffusion Lengths in $CH_3NH_3PbI_{3-x}Cl_x$ Perovskite Single Crystals

Fengying Zhang[ab], Bin Yang[bc], Yajuan Li[bc], Weiqiao Deng[*bc], Rongxing He[*a]

[a] Key Laboratory of Luminescence and Real-Time Analytical Chemistry (Southwest University), Ministry of Education, College of Chemistry and Chemical Engineering, Southwest University, Chongqing 400715, China.

[b] State Key Laboratory of Molecular Reaction Dynamics, Dalian Institute of Chemical Physics, Chinese Academy of Science, Dalian 116023, China.

[c] University of the Chinese Academy of Sciences, Beijing 10049, China

[*] Corresponding authors, Email: dengwq@dicp.ac.cn; herx@swu.edu.cn.

Analysis of the charge recombination and transfer processes:

As reported before, the recovery kinetics can be expressed as:[1]

$$\frac{dn}{dt} = An + Bn^2 \qquad (1)$$

where n is the photogenerated carrier density, and t is time. The rate constant A corresponds to the removal of either carrier to form an immobile species (a trap state), and B describes the free carrier recombination. When the perovskite is sandwiched between Au and Ga, the electron injection rate from the perovskite to the metal electrode can be defined as:[2]

$$K_{et} = \frac{2\pi}{h} \int_0^\infty dE \rho(E) \left| \overline{H(E)} \right|^2 \frac{1}{\sqrt{4\pi\lambda K_B T}} \exp\left(-\frac{(\Delta E + \lambda - E)^2}{4\lambda K_B T}\right) \qquad (2)$$

In Eq. (2) $\left| \overline{H(E)} \right|$ is the average electronic coupling between the perovskite valence band and the accepting metal states, $\rho(E)$ is the density of accepting states at the energy E relative to the valence band edge, and $\Delta E = E_v - E_c$ is the energy gap between the valence band of perovskite and the metal work function. It can be observed from Eq. (2) that the charge injection rate increases with an increasing energy gap. The charge injection efficiency η_{inj} is defined as $\eta_{inj} = \left[1 + f_g K_2 / K_1\right]^{-1}$, where $k_{1(2)}$ is the forward (backward) transfer rate constant, and f_g is a dimensionless factor related to the initial conditions.[2-3] To perform the calculation, η_{inj} can be estimated from the density of states:

$$\eta_{inj} \approx \left\{1 + f_g \left[\rho(E_c) / \rho(E_v)\right]\right\}^{-1} \qquad (3)$$

by using the following formula:

$$\rho(E) = N_1 \exp\left(\alpha E / k_B T\right) \qquad (4)$$

which expresses the density of states at the VBM (E_v) and Au (E_c). Assuming the difference of α can be ignored, Eq. (3) can be expressed as

$$\eta_{inj} \approx (1 + \lambda \exp(\beta \times \Delta E))^{-1} \quad (\lambda = \frac{N_1}{N_2} f_g, \quad \beta = \frac{\alpha}{k_B T}, \quad \lambda \text{ and } \beta \text{ are constants, } f_g$$

represents the geometry factor, N and α^{-1} are used to characterize the strength and distribution width of localized states in gap). Figure 4a shows the calculated η_{inj} as a function of the energy gap ΔE by assuming the value of $\lambda = 15$ and $\beta = -15$.[2] The injection efficiency increases with an increasing energy gap, whereas the slope first increases and then decreases. This behavior is ascribed to the dependence of the perovskite valence band on the rate constants.

Supplementary Figures
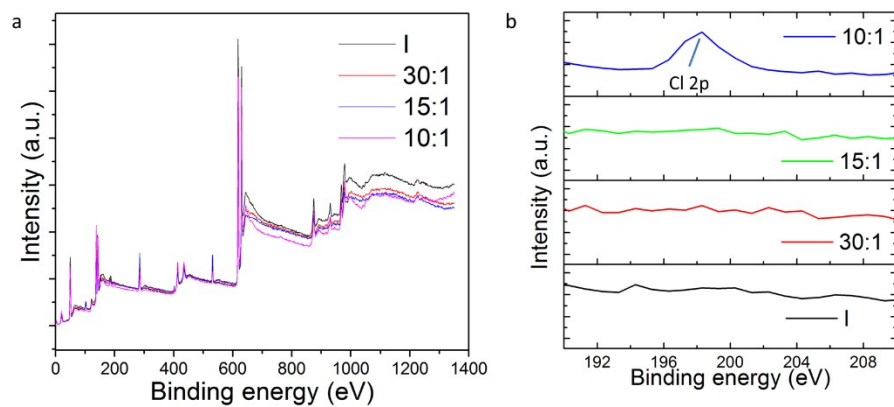
Fig. S1 XPS characterization of perovskite single crystals. (a) XPS survey spectrum of the top surface of the perovskite single crystals for all the four samples. (b) Cl2p core level XPS spectra of the perovskite single crystals, the characteristic peak binding energy of Cl2p 3/2 (198.9 eV) is indicated.
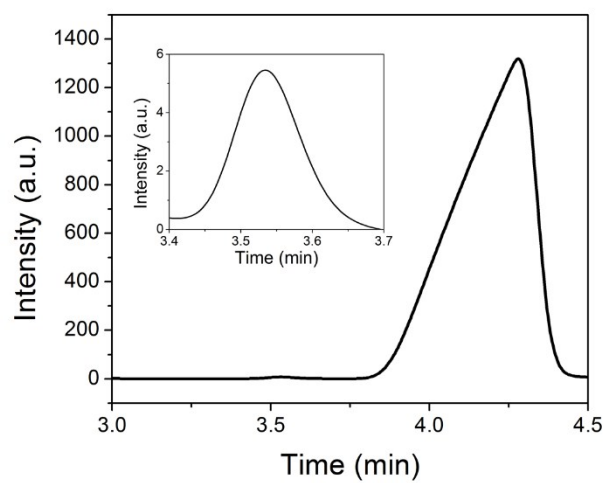
Fig. S2 Ion chromatographic analysis of I⁻ and Cl⁻ (inset), with specific retention times of 4.25 and 3.53 min, respectively.
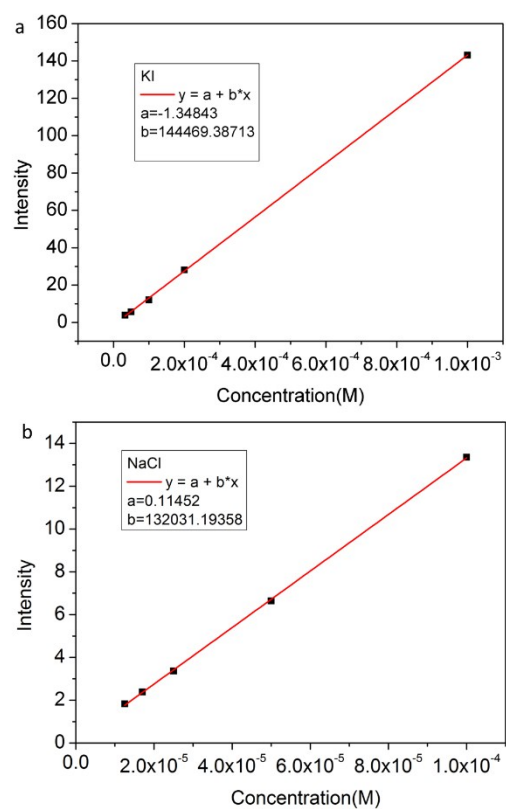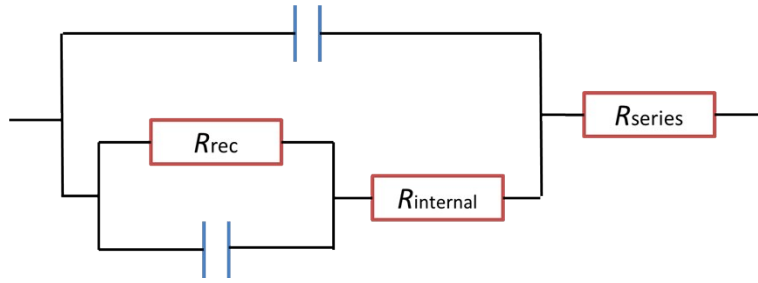
Fig. S3 Calibration curves for ion chromatography. Aqueous solutions containing different concentrations of iodide (a) or chloride (b) anion were analyzed by ion chromatography.
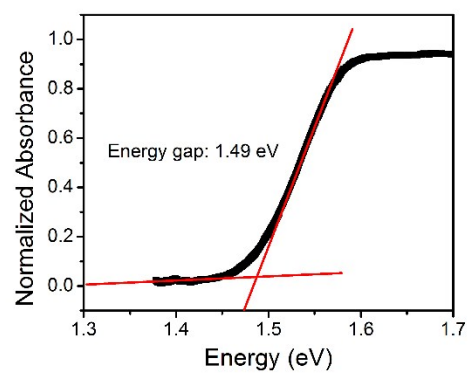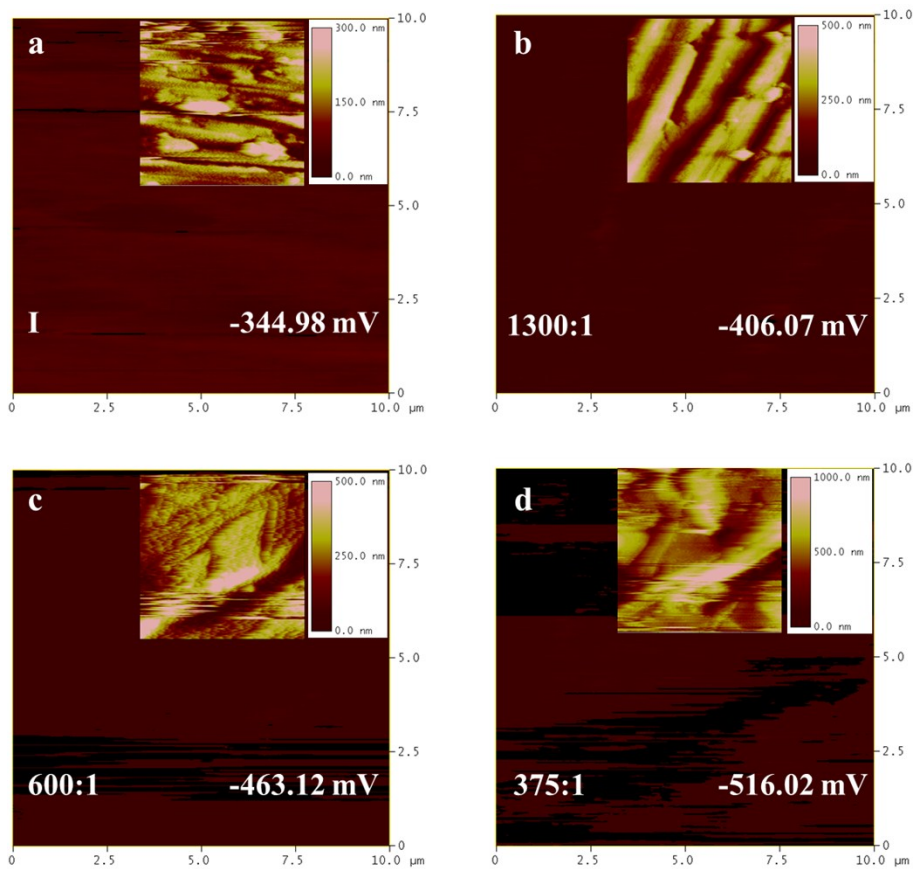
Fig. S4 (a) Calculation of the optical band gap for $CH_3NH_3PbI_3$ single crystal using the Tauc method.
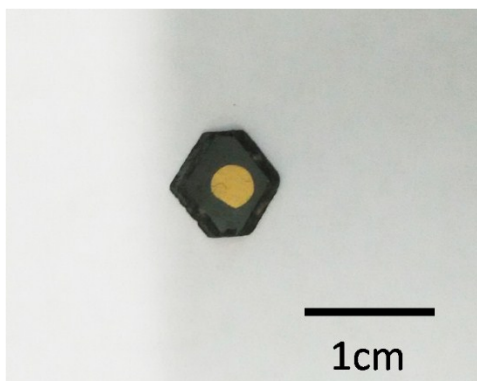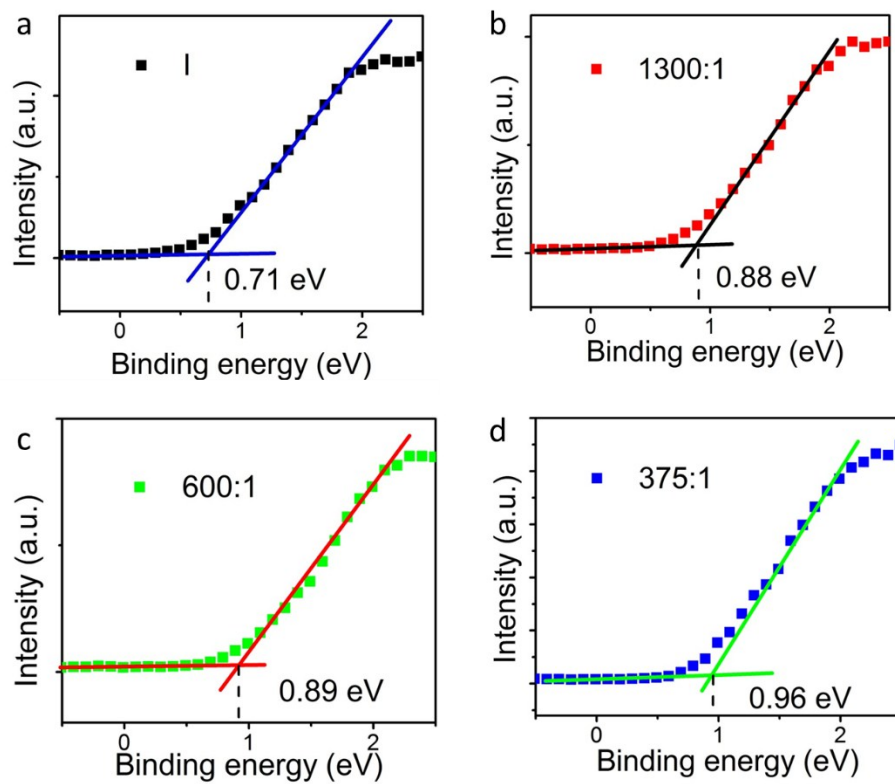
Fig. S5 Single crystal picture for the SCLC measurement.
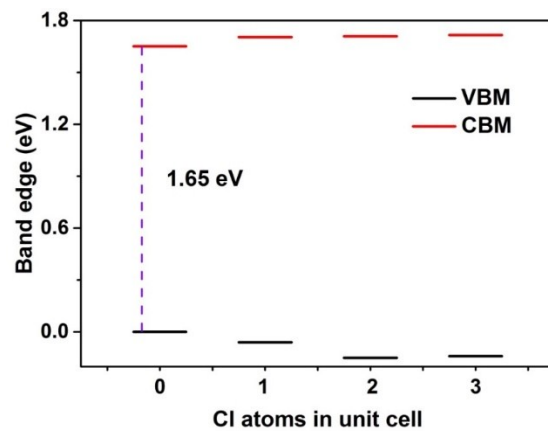
Fig. S6 Equivalent circuit used to fit the impedance spectroscopy measurement results.

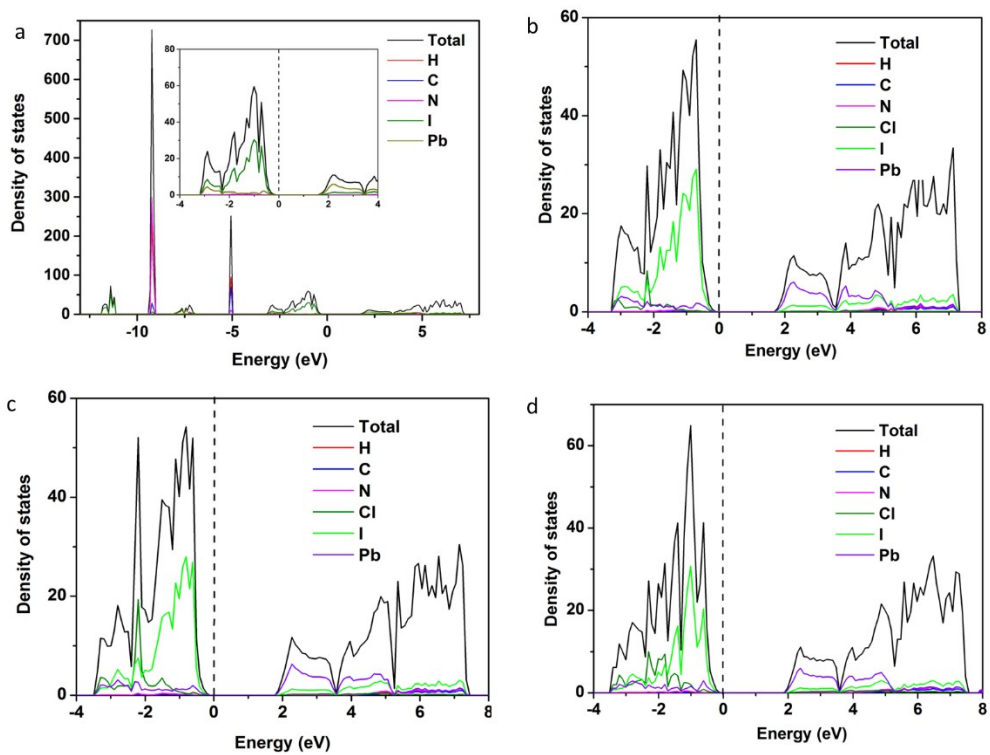**Fig. S7** KPFM characterization of perovskite single crystals. (a) KPFM images of local surface potentials of I, (b)1300:1, (c) 600:1 and (d) 375:1.

Fig. S8 Photoelectron spectroscopy spectra for (a) I, (b) 1300:1, (c) 600:1 and (d) 375:1.

Fig. S9 The band alignment of $CH_3NH_3PbI_3$ with and without Cl atom doping. The band gap of $CH_3NH_3PbI_3$ without Cl atom doping is 1.65 eV.

Fig. S10 The local density states (LDOS) of $CH_3NH_3PbI_3$ and $CH_3NH_3PbI_{3-x}Cl_x$. (a) LDOS of $CH_3NH_3PbI_3$. Inset: the LDOS around the Fermi level. (b)-(d) The LDOS around the Fermi level of $CH_3NH_3PbI_{3-x}Cl_x$ by doping 1~3 Cl atoms into the unit cell.

Table S1 Comparison of the trap-state density, carrier mobility and lifetime.

Performance parameters	Synthesis Method	Value	Characterization methods	Reference
trap densities	TSSG	3.6×10^{10} cm^{-3}	SCLC	[4]
	AVC	3.3×10^{10} cm^{-3}	SCLC	[5]
	ITC	1.4×10^{10} cm^{-3}	SCLC	[6]
	STL	3.82×10^{9} cm^{-3}	SCLC	[7]
	ITC	5.95×10^{9} cm^{-3}	SCLC	[8]
	ITC	1.8×10^{9} cm^{-3}	SCLC	[8]
	ITC	6.0×10^{8} cm^{-3}	SCLC	[9]
	ITC	1.3×10^{10} cm^{-3}	SCLC	Our result
Carrier mobility	TSSG	164 ± 25 cm^2 V^{-1} s^{-1}	SCLC	[4]
	TSSG	105 ± 35 cm^2 V^{-1} s^{-1}	Hall	[4]
	TSSG	24.0 ± 6.8 cm^2 V^{-1} s^{-1}	TOF	[4]
	ITC	67.2 ± 7.3 cm^2 V^{-1} s^{-1}	SCLC	[6]
	STL	121 ± 20 cm^2 V^{-1} s^{-1}	SCLC	[7]
	ITC	74 ± 12 cm^2 V^{-1} s^{-1}	SCLC	[7]
Lifetime	TSSG	95 μs (1 sun)	IS	[4]
	TSSG	198 μs (0.1 sun)	IS	[4]
	TSSG	82 μs (1 sun)	TPV	[4]
	TSSG	234 μs (0.1 sun)	TPV	[4]
	ITC	~300 μs (0.1 sun)	TPV	[7]
	STL	~400 μs (0.1 sun)	TPV	[7]
	ITC	127 μs (1 sun)	IS	Our result

References

1 J. S. Manser and P. V. Kamat, *Nat. Photon.*, 2014, **8**, 737-743.

2 J. Cai, N. Satoh and L. Han, *J. Phys. Chem. C*, 2011, **115**, 6033-6039.

3 Y. Li, X. Zhao, H. Li, D. Jin, F. Ma and M. Chen, *Mol. Phys.*, 2009, **107**, 2569-2577.

4 Q. Dong, Y. Fang, Y. Shao, P. Mulligan, J. Qiu, L. Cao and J. Huang, *Science*, 2015, **347**, 967-970.

5 D. Shi, V. Adinolfi, R. Comin, M. Yuan, E. Alarousu, A. Buin, Y. Chen, S. Hoogland, A. Rothenberger and K. Katsiev, *Science*, 2015, **347**, 519-522.

6 M. I. Saidaminov, A. L. Abdelhady, B. Murali, E. Alarousu, V. M. Burlakov, W. Peng, I. Dursun, L. Wang, Y. He, G. Maculan, A. Goriely, T. Wu, O. F. Mohammed and O. M. Bakr, *Nat. Commun.*, 2015, **6**, 7586.

7 Z. Lian, Q. Yan, T. Gao, J. Ding, Q. Lv, C. Ning, Q. Li and J.-l. Sun, *J.Am. Chem. Soc.*, 2016, **138**, 9409-9412.

8 Y. Liu, Z. Yang, D. Cui, X. Ren, J. Sun, X. Liu, J. Zhang, Q. Wei, H. Fan, F. Yu, X. Zhang, C. Zhao and S. Liu, *Adv. Mater.*, 2015, **27**, 5176-5183.

9 Y. Liu, Y. Zhang, Z. Yang, D. Yang, X. Ren, L. Pang and S. Liu, *Adv. Mater.*, 2016, **28**, 9204-9209.